DESIGN AND ANALYSIS OF COAXIAL GEAR-RACK POWER TRANSMISSION MECHANISM

Xinwen WU[1], Qing LIU[2,*]

This study proposes a coaxial gear-rack composite mechanism to replace traditional crank-connecting rod systems in engines, addressing heat loss and lateral pressure issues. The piston motion equations is established, and comparative analysis reveals 22.38% higher mechanical efficiency and 19.28% lower abrasion loss in the gear-rack system versus conventional mechanism. ADAMS simulations show the rotational speed of the engine increases by 65.97%, while ANSYS finite element analysis confirms gear meshing point stress compliance with strength requirements. This research provides foundational support for developing energy-efficient power transmission systems in high-performance sports vehicular applications, demonstrating performance improvements over traditional designs.

Keywords: Engine; Numerical simulation; Crank connecting rod; Transmission efficiency.

1. Introduction

Since its birth, the crank linkage power transmission mechanism has been widely used in various fields such as automobile, aerospace and so on [1-6], with its simple structure, reliable steering, easy to control the phases in each cylinder body, and capable of adapting to a variety of high temperatures and other working environments. However, as the engine was developed over time, researchers discovered that the conventional crank linkage power transmission mechanism there are still many unavoidable defects [7,8]: (1) In traditional crankshaft connecting rod mechanisms, a considerable lateral pressure is generated between the piston assembly and the cylinder wall, which leads to increased wear between them and significantly reduces their service life. (2) For sports cars that pursue motion performance, the larger the ratio of crank to link length is, the shorter the piston stroke will become and the engine speed will increase, but the engine torque output will decrease significantly, resulting in low mechanical efficiency [9].

The rack and pinion mechanism has high mechanical transmission efficiency and can effectively reduce the cylinder wall pressure. Therefore, some researchers at home and abroad began to carry out in-depth exploration of the rack and pinion

[1] PhD, Dept. of Engineering Mechanics, China University of Mining and Technology-Beijing, China, e-mail : 18281220586@163.com
[2*] Eng., Dept. of Engineering Mechanics, China University of Mining and Technology-Beijing, China, e-mail: liuqing1016821@163.com) (corresponding author)

transmission mechanism [10,11]: Zhou Weihua used the symmetry principle to design a single-gear double rack and pinion transmission mechanism, which is used in the regulating valve to ensure that the pressure of the internal flow field is more uniform [12]; Peng Zhenhua carry out mechanical analysis to gear and long annular rack pinion transmission mechanism, and explore solutions to how to make the mechanism more stable [13]; Richard D. Rucker invented a two-stroke engine using internal cycloid rack and pinion mechanism drive, and theoretically verified that it effectively reduces the cylinder wall pressure [14]; Niu Ziru designed and studied the variable ratio gear set, which improved the portability and sensitivity of the transmission mechanism [15]; However, at present, most of these mechanisms still have dead point zones or non-meshing zones when the gas detonation force in the cylinder is at its maximum, and they do a lot of ineffective work

Based on the aforementioned, this paper designs and analyzes a new coaxial gear-rack transmission mechanism. It avoids the dead point zone when the gas deflagration force in the cylinder is the maximum, which leads to increase its effective work and improve its mechanical transmission efficiency. At the same time, the stroke of the piston is relatively large and the rotational speed of the engine is relatively high, which is conducive to enhancing the motion performance of the sports car.

2. Principle of Operation

Coaxial double gear-rack transmission mechanism shown in Fig.1, the gear device has a pair of coaxial gears, to ensure that the front and rear gears have the same rotational speed; rack device consists of the upper rack meshing with the front side of the large gears and the rear side of the small gears meshing with the lower rack, in which the lower rack connected to piston in the cylinder body through the pin and the upper rack hinged with the crank, so that the crank can be driven to rotate around the stator shaft. Additionally, the crank's and the gear set's rotation axes are parallel to one another.

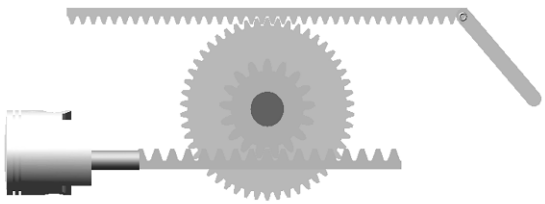

Fig.1 Mechanism principle

When the gas in the cylinder does work through expansion, the piston pushes the lower rack to move horizontally to the right, the lower rack meshes with the

rear gear and drives the coaxial gear set to rotate counterclockwise, the front gear meshes with the upper gear, the counterclockwise rotation of the front gear drives the upper rack to do planar motion, which drives the crank to rotate counterclockwise; when the work done by the gas in the cylinder is 0, the piston continues to move to the right for a certain distance due to the inertia; until the speed of the piston is 0. When the work done by the gas in the cylinder is 0, the piston continues to move to the right for a certain distance due to inertia; until the speed of the piston becomes 0, the crank will still rotate counterclockwise due to inertia, which will make the upper rack do planar motion and drive the coaxial gear set to rotate clockwise, which will drive the lower rack and the piston to move horizontally to the left, realizing the process of exhausting the gas; and then repeat the compression process of the cylinder gas, thus completing the cycle once, realizing the change from the straight-line movement of the piston to the rotation of the crank output shaft.

In the cylinder gas release of deflagration force at the moment of maximum, the angle between the connecting rod of traditional crank linkage mechanism and the horizontal plane is small, deflagration force have too force arm small on the crank rotary axis, the effective output of work is less. On the contrary, in the coaxial double gear-rack transmission mechanism, the deflagration force is passed by the piston to the upper rack, at this time, the upper rack has a larger force arm of the output shaft, greatly increasing the effective output of work, and at the same time to avoid the generation of the entire cycle of the dead spot area.

3. Velocity Equation of the Piston

Coaxial double gear-rack transmission mechanism sketch shown in Fig.2,

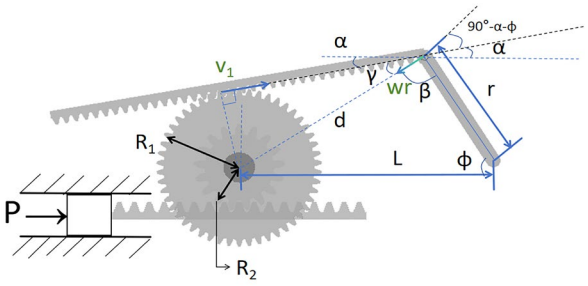

Fig.2 Gear-rack power transmitting mechanism

The linear velocity at the articulation of the crank and upper rack is ωr, the velocity at the point of upper rack with the front gear can be obtained from the velocity projection method:

$$v_1 = \omega r \cos\left(90° - \phi - \alpha\right) = \omega r \sin(\phi + \alpha) \tag{1}$$

From Fig.2:

$$\alpha = 180° - \phi - \beta - \gamma \tag{2}$$

And it is obtained from the geometric relation:

$$\begin{cases} \dfrac{d}{\sin\phi} = \dfrac{L}{\sin\beta} \\ \sin\gamma = \dfrac{R_1}{d} \end{cases} \tag{3}$$

The angle between the horizontal line and the upper rack α is represented as follows.

$$\alpha = 180° - \phi - \sin^{-1}\left(\frac{L\sin\phi}{d}\right) - \sin^{-1}\left(\frac{R_1}{d}\right) \tag{4}$$

Equation.(4) is then brought into Eq.(1) to obtain the linear velocity at the meshing point of the upper rack and front gear:

$$v_1 = \omega r\left(\frac{L\sin\phi}{d}\cdot\sqrt{1-\frac{R_1^2}{d^2}} + \frac{R_1}{d}\cdot\sqrt{1-\frac{L^2\cdot\sin^2\phi}{d^2}}\right) \tag{5}$$

Expanding the root sign of Eq.(5) using Taylor's formula and omitting the higher order terms, the velocity equations of the coaxial gear set and piston in generalized coordinates can be obtained by using the properties of coaxial gear linear velocity:

$$v_1 = \omega r\left(\frac{L\sin\phi + R_1}{d} - \frac{R_1 L(R_1 + L)\sin\phi}{2d^3}\right) \tag{6}$$

$$v_p = \omega r\cdot\frac{R_2}{R_1}\cdot\left(\frac{L\sin\phi + R_1}{d} - \frac{R_1 L(R_1 + L)\sin\phi}{2d^3}\right) \tag{7}$$

In summary, it can be seen when the crank rotary radius is certain, the speed of the piston can be reduced by reducing R_2/R_1. In other words, without increasing the eccentricity, the piston stroke can be reduced by using a coaxial gear set with an appropriate radius of gyration ratio, which effectively reduces friction loss and extends the service life of the piston and the pulling cylinder.

4. Comparison of Power Transmission Performance

4.1 Comparative Analysis of the Mechanical Transmission Efficiency

A sketch of the conventional crank connecting rod power transmission mechanisms is shown in Fig.3. The mechanical transmission efficiency of the conventional crank linkage is calculated as follows [15]:

$$\eta = 1 - \frac{dw_1/dt + dw_2/dt + dw_3/dt + dw_4/dt}{dw/dt}$$
$$= 1 - \frac{\sqrt{r^2 - e^2\sin\theta}[f_1 e\sin^2\theta + (f_2 r_2 + f_3 r_3)] + e\cos\theta[f_1 e\cdot\sin^2\theta + (f_3 r_3 + f_4 r_4)]}{e\sin\theta\cos\theta\cdot(\sqrt{r^2 - e^2\sin^2\theta} + e\cdot\cos\theta)}$$
$$(\Delta\theta < \theta < \sin^{-1}\frac{r}{e}) \tag{8}$$

The friction loss rate contributed by the moving pair of the piston and the inner wall of the cylinder:

$$\delta = \frac{dw_1/dt}{dw/dt} = \frac{Pe\sin^2\theta(\frac{1}{\cos\theta} + \frac{1}{\sqrt{r^2 - e^2\sin^2\theta}})}{Pe\sin\theta(1 + \frac{e\cos\theta}{\sqrt{r^2 - e^2\sin^2\theta}})} \tag{9}$$

The mechanism is in the dead point region when $\eta = 0$, and the critical point should be in the region around = 0; Eq.(9) can be obtained by bringing $\eta = 0$ into Eq.(8):

$$\Delta\theta = \frac{r(f_2 r_2 + f_3 r_3) + e(f_3 r_3 + f_4 r_4)}{e\cdot(r + e)} \tag{10}$$

During the crank rotating, θ will increase from 0 to $\sin^{-1}(r/e)$, and then from $\sin^{-1}(r/e)$ to 2π (this process is the same as decreasing from $\sin^{-1}(r/e)$ to the 0 state), and the change in η is completely symmetric.

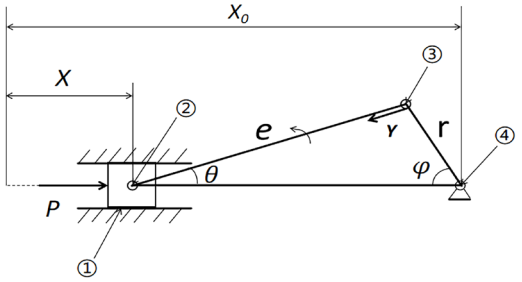

Fig.3 Crank connecting rod diagram

Obviously, if the dead point interval is shorter, the more effective work will be done and the transmission efficiency will be higher. In order to facilitate simulation and analysis, the relevant parameters of the crank linkage are set as shown in Tab.1 below:

Table 1

Crank connecting rod relevant parameter

Parameter	Value	Parameter	Value
Linkage length *e*/mm	90	①friction coefficient f_1	0.10

Crank length r/mm	35	②friction coefficient f_2	0.05
②Pin radius r_2/mm	15	③friction coefficient f_3	0.10
③Pin radius r_3/mm	30	④friction coefficient f_4	0.05
④Pin radius r_4/mm	30		

The relevant parameters of Tab.1 are brought into Eq.(8) and integrated to calculate the average transmission efficiency:

$$\eta=\frac{\int_{0.04764}^{0.3992}\left(1-\frac{\sqrt{1225-8100\sin^2\theta}\left(9\sin^2\theta+3.75\right)+90\cos\theta\left(9\sin^2\theta+4.5\right)}{90\sin\theta\cos\theta\left(\sqrt{1225-8100\sin^2\theta}+90\cos\theta\right)}\right)d\theta}{0.3992-0.04764}=60.5\% \tag{11}$$

Similarly, the relevant parameters of Tab.1 are brought into Eq.(9) and integrated to calculate the average friction loss rate between the piston and the inner wall of the cylinder:

$$\delta=\frac{dw_1/dt}{dw/dt}=\frac{\int_{0.04764}^{0.3992}\frac{Pe\sin^2\theta\left(\frac{1}{\cos\theta}+\frac{1}{\sqrt{r^2-e^2\sin^2\theta}}\right)}{Pe\sin\theta\left(1+\frac{e\cos\theta}{\sqrt{r^2-e^2\sin^2\theta}}\right)}d\theta}{0.3992-0.04764}=22.98\% \tag{12}$$

The diagram of the coaxial gear-rack power transmitting mechanism is shown in Fig.4, and the friction loss work of each moving pair is deduced below to calculate the mechanism transmission efficiency.

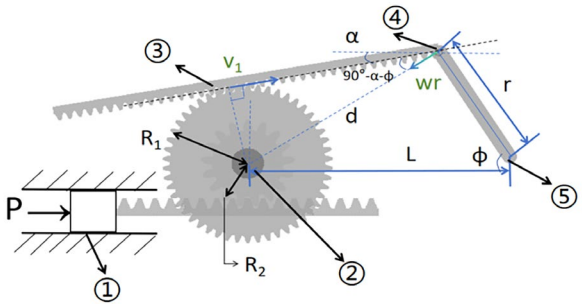

Fig.4 Coaxial gear-rack power transmitting mechanism diagram

(1) Gas input work in the cylinder:

$$dW=PR_2d\theta \tag{13}$$

(2) Friction loss power between the piston and the moving side of the cylinder:

$$dW_1=f_{s1}R_2\cdot P\tan\beta\cdot d\theta=f_{s1}R_2\cdot\frac{P\rho_2}{r_2}d\theta \tag{14}$$

(3) Friction loss power in the gear shaft rotating pair:

$$dW_2 = f_{s2} \tan\beta (PR_2 + P\frac{R_2}{R_1} \cdot R_1) d\theta \tag{15}$$

(4) Friction loss power at the meshing point of the rack and pinion set:

$$\begin{aligned} dW_3 &= P\sin\varphi_f \cdot v_{1+2} dt = P\sin\varphi_f \cdot \omega_1 \rho_{1+2} dt = P\sin\varphi_f \cdot \rho_{1+2} d\theta \\ &= P(\rho_1 + \rho_2)\sin\varphi_f d\theta = P(\rho_1 + \rho_2)\sin\left[\tan^{-1} f_{s3}\right] d\theta \end{aligned} \tag{16}$$

(5) Friction loss power of the rotating pair at the hinge between the upper rack and crank:

$$\begin{aligned} dW_4 &= f_{s4} \cdot \left(\frac{R_2 P}{R_1}\right) \cdot \sin(\varphi + \alpha) ds = f_{s4} \cdot \left(\frac{R_2 P}{R_1}\right) \cdot [\sin(\varphi + \alpha)\omega r] dt \\ &= f_{s4} \cdot \left(\frac{R_2 P}{R_1}\right) v_1 dt = f_{s4} \cdot \left(\frac{R_2 P}{R_1}\right) R_1 d\theta = f_{s4} P R_2 d\theta \end{aligned} \tag{17}$$

(6) Friction loss power of the crank rotating pair:

$$dW_5 = f_{s5} \cdot \left(\frac{R_2 P}{R_1}\right) \cdot \sin(\varphi + \alpha) ds = f_{s5} P R_2 d\theta \tag{18}$$

In summary, the mechanical transmission efficiency of the coaxial gear-rack power transmitting mechanism can be deduced:

$$\begin{aligned} \eta &= 1 - \frac{dW_1/dt + dW_2/dt + dW_3/dt + dW_4/dt + dW_5/dt}{dW/dt} = \\ &1 - \frac{\frac{f_{s1}\rho_2 R_2}{r_2} + 2f_{s2}R_2 + f_{s3}(\rho_1 + \rho_2)\sin\left[\tan^{-1} f_{s3}\right] + (f_{s4} + f_{s5})R_2}{R_2} \end{aligned} \tag{19}$$

The friction loss rate contributed by the moving pair of the piston and the inner wall of the cylinder:

$$\delta = \frac{dw_1/dt}{dw/dt} = \frac{f_1 R_2 \frac{P\rho_2}{r_B} d\theta}{PR_2 d\theta} = f_1 \frac{\rho_2}{r_2} \tag{20}$$

The relevant parameters affecting the mechanical transmission efficiency of the mechanism are set as shown in Table2 below for simulation analysis:

Table 2

Coaxial Gear-rack mechanism relevant parameter

Parameter	Value	Parameter	Value
Radius of front gear pitch circle R_1/mm	90	①friction coefficient f_{s1}	0.10

Radius of rear gear pitch circle R_2/mm	30	②friction coefficient f_{s2}	0.05
Radius of rear gear base circle r_2/mm	27	③friction coefficient f_{s3}	0.05
Radius of front gear meshing point ρ_1 /mm	12	④friction coefficient f_{s4}	0.10
Radius of front gear meshing point ρ_2 /mm	10	⑤friction coefficient f_{s5}	0.05

The parameters in the table are brought into Eq.(19) and Eq.(20):

$$\eta = 1 - \frac{0.1 \cdot 1 \cdot 3 / 2.7 + 0.05 \cdot 9 + 0.05 \cdot 2.20 \cdot \sin\left[\tan^{-1} 0.05\right] + 0.10 \cdot 3}{3} = 82.88\% \quad (21)$$

The average friction loss rate between the piston and the wall of the cylinder:

$$\delta = 0.1 \times \frac{10}{27} = 3.70\% \quad (22)$$

As a result, compared to the conventional crank linkage mechanism, the mechanical transmission efficiency of the coaxial double rack-pinion power transmission mechanism increases:

$$\Delta\eta = 82.88\% - 60.5\% = 22.38\% \quad (23)$$

In this paper, the average friction loss rate between the piston and the inner wall of the cylinder is taken as the measurement form of piston wear. Therefore, compared with the traditional crank connecting rod mechanism, the wear of this new type of mechanism is reduced by:

$$\Delta\delta = 22.98\% - 3.70\% = 19.28\% \quad (24)$$

In conclusion, not only has the mechanical transmission efficiency of the coaxial double rack and pinion mechanism been significantly increased, but also the wear between the piston assembly and the cylinder wall has been reduced, which greatly extending the service life of the piston rings and the pull cylinder.

4.2 Comparative Simulation Analysis of Two Mechanism Strokes and Rotational Speed

The piston stroke is a key factor affecting the power output of the engine. A small stroke means that the engine piston can make more reciprocating movements within a unit of time, that is to say, it is easier to reach a higher rotational speed. A large stroke means that the piston has a longer distance to accelerate, and thus can output high torque at a low rotational speed. In sports car design, a higher rotational speed is conducive to enhancing its sports performance in order to meet the needs of customers.

In this paper, ADAMS dynamics simulation software is used to simulate and analyze the traditional crank link and coaxial double rack-pinion power transmission mechanism respectively [17-19].

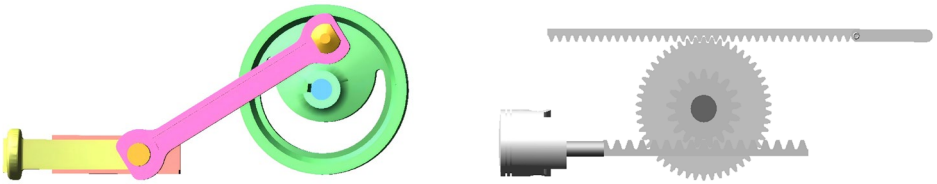

(a) Crank connecting rod dynamical model (b) Coaxial gear-rack dynamical model

Fig.5 The dynamic model established in ADAMS

4.2.1 Dynamics Simulation of Conventional Crank Connecting Rod

Firstly the traditional crank connecting rod model is assembled as Fig.5(a) and imported into ADAMS. Then, the technical parameters of the conventional crank connecting rod are set as shown in Tab.1 above. In addition, the material coefficients and mass of each component are defined in this model [20-22].

(1) Constraint setting: first of all, it is necessary to increase the corresponding motion vice constraints in each motion component: a translation pair is set between the piston and the ground, a rotation vice is set between the connecting rod and the piston to establish, a rotation vice is set between the crank and the connecting rod, and another rotation vice fixed in the rotary axis is set between the crank and the ground.

(2) Driving force setting: when applying driving force, in order to facilitate the analysis, this paper adopts the reverse analysis method: the piston is driven to move horizontally through the rotation of the crank. Therefore, the driving force is set on the crank rotary axis, in other words, the driving force is set on the rotating vice between the crank and the ground, and the STEP function is utilized to control the rotational speed of the crank. At this time, the crank will keep the rotational speed of 3141.5 r/min after acceleration. Meanwhile, the simulation time is set to be 2 s. Simultaneously, the step size is set to be 2000.

4.2.2 Dynamics simulation of coaxial gear-rack mechanism

The relevant technical parameters of the coaxial rack and pinion crank mechanism are shown in the Table3 as below:

Table 3

Major parameter of coaxial gear-rack mechanism

Parameter	Value	Parameter	Value
Gear module m_1	1	Gear pressure angle	20°
Front gear teeth z_1	50	Gear set materials	20Cr2Ni4A 钢
Rear gear teeth z_2	17	Tooth hardness	$\geq 60HRC$
Crank length r	35mm		

(1)Constraint setting: The whole power transmission mechanism is divided into frame, piston, lower rack-rod assembly, coaxial gear set, upper rack-crank assembly, and high-speed rotating shaft. The parts are merged into each assembly, and the corresponding rotational constraints are added between the corresponding moving parts: the fixed vices are set between the piston and the ground, between the piston rod and the ground, and between the lower rack and the ground respectively; a translation vice is set between the lower rack and the ground; a rotational vice is set between the front and rear gears and the ground, and a coupling vice is set between the front gear and rear gear; a rotational vice is set between the upper rack and the crank; another rotational vice is set between the crank and the earth. After adding the kinematic pair, it is necessary to add contact constraints between the rack and pinion. According to the Hertz contact theory, the contact stiffness between the rack and pinion is correctly calculated [23].

(2) Driving force setting: similar to the driving force setting applied to the traditional crank connecting rod, this paper adopts the reverse analysis method: through the high-speed rotation of the crank to drive the rotation of the gear set, which in turn drives the reciprocating motion of the piston. In order to make the crank rotate at a high speed, the driving force is applied to the rotating vice between the crank and the ground, and the STEP function is utilized to control the rotational speed of the crank. At this time, the crank will keep the rotational speed of 3141.5 r/min after acceleration as conventional mechanism. Similarly, the simulation time is set to be 2 s. Likewise, the step size is set to be 2000.

4.2.3 Simulation Results and Analysis

The displacement and speed curves of the piston are shown below:

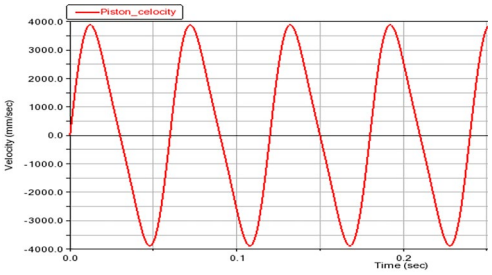

(a) Velocity of the crank connecting rod

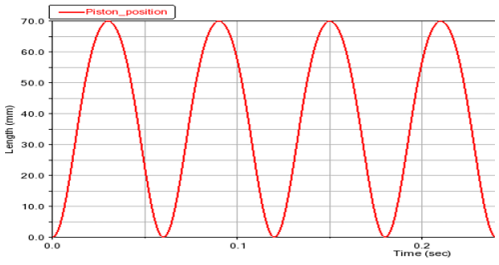

(b) Position of the crank connecting rod

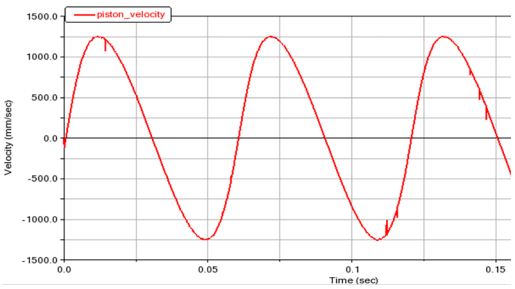

(c) Velocity of the coaxial gear-rack

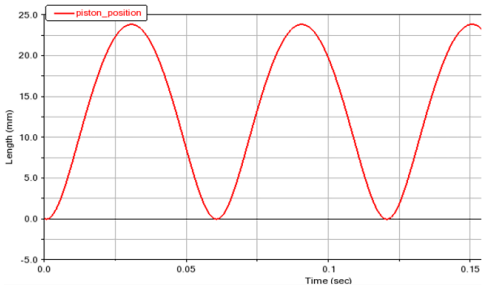

(d) Position of the coaxial gear-rack

Fig.6 Curve diagram of the simulation results

From the curve diagram of the crank connecting rod as Fig.6(a) and Fig.6(b), it can be seen that when the eccentricity of the crankshaft is 35 mm, the stroke of the piston reaches 70 mm, and the maximum speed of the piston reaches 3886 mm/s; in addition, the displacement curve and the velocity curve are smooth and complete, and the whole of them show the motion curves with approximate sinusoidal function which verifies the motion characteristics of the piston, and proves that the piston can complete the reciprocating motion in a smooth way.

As can be seen from Fig.6(c), the rack and pinion will produce vibration when meshing, gear speed will produce small fluctuations, but does not affect the piston's movement characteristics, the piston speed curve as a whole is still sinusoidal curve. As shown in Fig.6(d), the piston stroke of the coaxial rack and pinion set mechanism is only 23.82 mm, which is smaller than that of the traditional crankshaft connecting rod.

$$\Delta s = \frac{70 - 23.82}{70} \times 100\% = 65.97\% \tag{25}$$

The rotational speed of the engine crankshaft and the piston stroke satisfy the following relationship:

$$\mathrm{n} = \frac{60 v_p}{2s} \tag{26}$$

From this, it can be known that if the average speed of the piston v_p and the length of the crankshaft r in the two mechanisms are guaranteed to be the same, compared with the traditional crankshaft connecting rod mechanism, the coaxial rack and pinion mechanism can theoretically increase the rotational speed of the engine by 65.97%, making it easier to reach high speeds and ensuring the motion performance of the sports car at high speeds.

5. Transient Dynamics Analysis

During the overall motion of the coaxial double gear-rack power transmission mechanism, the rack and pinion generates vibration during the meshing process, so it is necessary to analyze the transient dynamics in the reciprocating motion of

the rack and pinion. In this paper, ANSYS is used to analyze the stresses in its motion process and to ensure that the rack and pinion structure meets the material requirements.

5.1 Analysis of Hazardous Stress Points

As the front gear indexing circle radius R_1 is larger than the back gear indexing circle radius R_2, in the whole transmission process, the impact force at the meshing point of the rear gear and the lower rack will be significantly larger than the impact force at the meshing point of the front gear and the rack. Therefore, at the instant of rack and pinion mesh commutation and when the cylinder gas generates the maximum burst pressure, the maximum stress point of the entire mechanism is in the area between the rear gear and the lower rack. When the rack perpendicular to the crank, exactly the maximum stress point is in the area between the front gear and rack (that is, at this moment, the crank rotates at a uniform speed required centripetal force which is all provided by the upper rack, and the positive pressure between the front gear and the upper rack reaches the maximum).

5.2 Finite Element Analysis Settings

In actual working conditions, sliding friction will occur between the pinion and rack and there will be a certain friction resistance. Therefore, the contact type of the pinion and rack is set to frictional contact, and the friction coefficient is set to 0.1

The model was meshed: tetrahedral mesh was used, and the algorithm was patch conformal method. At the same time, mesh encryption is taken at rack and pinion contact points.

Next the constraints in the model are defined, which are set different in the three danger points: (1) At the instant of rack and pinion mesh commutation: The lower rack is provided with a translation pair, specifically, the displacement in the x direction is free, and the displacement in the y and z directions is 0. Since the speed of the rack is 0 when the mesh is reversed, the gear will continue to rotate a small angle due to inertia, so it is necessary to apply a rotating pair to the gear and define a 2° rotation within 1s.

(2) At the instant of maximum cylinder gas deflagration power: The lower rack moves horizontally along the x axis. As in the first case, the free displacement in the x direction is set, and the displacement to 0 in the y and z directions is set.

(3) When upper rack and crank are perpendicular to each other: The upper rack do the general plane motion, so we need to apply displacement constraints, the free displacement in the x and y direction is set, and the displacement to 0 in the z directions is set.

Finally, it is necessary to apply loads to the model. Since the force on the upper rack is provided by the crankshaft, the load is applied at the articulation between the upper rack and the crankshaft, and the load size is output by ADAMS.

5.3 Solution Results

The calculation is completed by the LDS solver of ANSYS. The display of the calculation results depends on the strain diagram and stress distribution diagram. Moreover, the stress situation of various working conditions can be obtained through the cloud diagram.

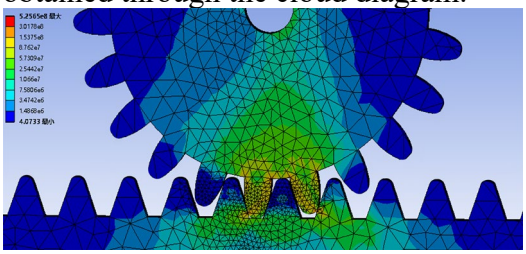

(a) The lower rack and rear gear at the instant of rack and pinion mesh steering

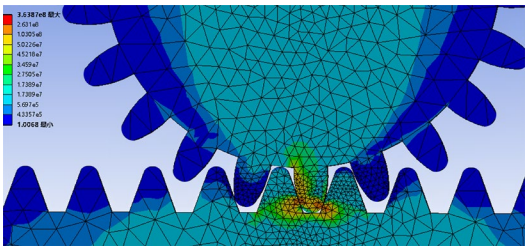

(b) The teeth at the instant of maximum cylinder gas deflagration power

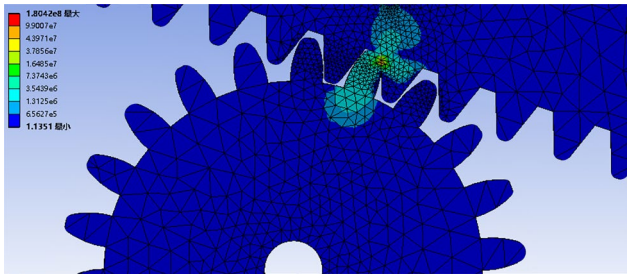

(c) Between upper rack and front gear when upper rack and crank are perpendicular to each other

Fig.7 Stress distribution pattern

A finite element model is set in the lower rack and pinion meshing process [24], simulation analysis shows that: when the rack and pinion meshing direction is turned, the maximum stress suffered by the wheel teeth is 525.65 MPa; at the instant when the deflagration force of the cylinder gases is maximized, the maximum stress suffered by the wheel teeth is 363.87 MPa.

Simulation of the upper rack and front gear meshing process shows that, when the upper rack and crank are perpendicular to each other, the maximum stress point is generated between the upper rack and front gear. At this moment, the centripetal force required for the crank to rotate at a uniform speed is all provided by the upper rack, and the positive pressure between the upper rack and the front gear reaches the maximum. From the analysis of Fig.8, it can be seen that the maximum stress on the gear teeth at this instant is 180.42 MPa.

5.4 Fatigue Strength Verification of Rack and Pinion

During the reciprocating motion of the rack and pinion, the impact force and positive pressure on the gear teeth also change cyclically, and eventually the fatigue limit is reached under the action of countless alternating stresses, so it is necessary to verify the fatigue strength at the hazardous cross-section.

In the above three hazardous working conditions, the cycle characteristics of the gear teeth are zero cycle, i.e. pulsating cycle. Therefore the form of failure of rack and pinion transmission is tooth contact fatigue pitting [25]. The following verification of fatigue strength of rack and pinion under pulsating cyclic stresses is carried out [26]:

Stress amplitude：

$$\sigma_a = \frac{\sigma_{\max} - \sigma_{\min}}{2} \tag{27}$$

Average stress：

$$\sigma_m = \frac{\sigma_{\max} + \sigma_{\min}}{2} \tag{28}$$

Fatigue strength safety factor：

$$S = \frac{K'_N \sigma_{-1}}{\frac{k_\sigma}{\varepsilon_\sigma \beta_m}\sigma_a + \varphi_\sigma \sigma_m} \geq [S] \tag{29}$$

Throughout the process, the wheel teeth will be subjected to a maximum stress of 525.65 MPa when the rack and pinion meshes are turned. The fatigue safety factor of the rack and pinion is calculated at this instant after bringing in the mechanical property parameters of $20Cr_2Ni_4A$ [27]:

$$\begin{aligned} S &= \frac{K'_N \sigma_{-1}}{\frac{k_\sigma}{\varepsilon_\sigma \beta}\sigma_a + \varphi_\sigma \sigma_m} = \frac{1.54 \cdot (1483 \cdot 0.4)}{\frac{1.60 \cdot 262.83}{0.83 \cdot 1} + 0.25 \cdot 262.83} \\ &= 1.59 > [S] = 1.50 \end{aligned} \tag{24}$$

Wheel teeth at the point of maximum stress meet the fatigue strength requirements, so the transmission mechanism is safe and reliable.

6. Conclusions

(1) This paper proposes a power transmission mechanism driven by a coaxial double rack and pinion, instead of the traditional crank linkage mechanism, the rack and pinion has a larger force arm on the output shaft at the moment of the maximum deflagration force, which greatly increases its effective work, thus increasing the mechanical transmission efficiency. At the same time, the friction loss is effectively reduced, and the service life of the piston and the pulling

cylinder can be prolonged.

(2) Under the premise of the crank rotary radius remains unchanged, the speed of the piston can be reduced by reducing the ratio of the indexing circle radius of the rear gear and the front gear, thus reducing the piston stroke, making it easier to reach high speeds and ensuring the motion performance of the sports car at high speeds.

(3) Theoretical calculations and dynamics simulation analyses carried out for the two mechanisms of the same model show that: compared with the traditional crank connecting rod, the mechanical transmission efficiency of the coaxial double gear-rack power transmission mechanism increases by 22.38% and the rotational speed of the engine increases by 65.97%.

(4) The transient dynamics simulation of the coaxial double gear-rack power transmission mechanism is carried out, and the stress maps are obtained under the three dangerous working conditions: the instant of rack and pinion mesh steering, the instant of maximum cylinder gas deflagration power, and the instant of upper rack and crank are perpendicular to each other, respectively, and it is analyzed that the maximum stress suffered by the gear teeth is 525.65 MPa, which meets the requirements of fatigue strength.

NOMENCLATURE

d	distance between the crank and the upper rack articulation point to the gear shaft, $d = \sqrt{r^2 + L^2 - 2rL\cos\varphi}$, mm
dw/dt	crank connecting rod device intake power
dw_1/dt	friction loss power of piston device and cylinder wall translation pair at ①
dw_2/dt	connecting rod and piston rotation pair at ②
dw_3/dt	friction loss power of the crankshaft and the connecting rod rotation pair at ③
dw_4/dt	friction loss power of the crankshaft rotation pair at ④
e	connecting rod length, mm
f_1	friction coefficient of the piston and cylinder wall
f_2r_3	friction circle radius of rotation pair ②
f_3r_3	friction circle radius of rotation pair ③
f_4r_4	friction circle radius of rotation pair ④
f_{s1}	friction coefficient of the piston moving vice
f_{s2}	friction coefficient of gear shaft rotary vice
f_{s3}	friction coefficient of moving vice at the rack and pinion meshing point
f_{s4}	friction coefficient of the rotation pair at the hinge between the upper rack and the crank
f_{s5}	friction coefficient of the crank rotary vice
K_N'	part life factor
K_σ	effective stress concentration factor
L	distance between the crank rotary axis and the gear shaft, mm
n	rotational speed of the crank, r / min
P	gas deflagration force in cylinder, N
R_1	pitch radius of the front gear, mm

R_2 pitch radius of the rear gear, mm
r rotary radius of the crank, it can also be the crankshaft eccentricity, mm
r_B radius of the rear gear base circle, mm
[s] permissible fatigue safety factor for parts
v_1 upper rack and front gear engagement point speed, m/s
v_2 under rack and rear gear engagement point speed, m/s
v_p horizontal speed of the piston.
α angle between the horizontal line and the upper rack
β angle of two lines from on the crank to the gear shaft and from the rack articulation point to the crank rotary axis
β_m surface stress state factor
γ angle of the line from the upper rack to the gear shaft and the crank on the rack articulation point
δ Wear and tear consumption rate
ω angular velocity of the crank, $\omega = 2\pi \mathrm{n}$, rad / s
ω_1 angular velocity of the crank rotation, rad/s
ϕ crank angle, when the crank rotates at a constant speed, $\phi = \omega t$
φ_σ equivalent coefficient of average stress converted to stress amplitude
φ_f friction angle, and to meet $\varphi_f = \sin^{-1} f_{s3}$
σ stress at gear meshing point
σ_{-1} fatigue limit of materials under symmetric cyclic stress
ρ_1 mean radius of curvature of the front gear meshing point, mm
ρ_2 mean radius of curvature of the rear gear meshing point, mm
ε_σ absolute size factor
θ angle of the connecting rod and the horizontal plane, $0.04764 \le \theta \le 0.3992$

R E F E R E N C E S

The references will be written in small letters, 10 pts, numbered by [1], [2], etc., in the order of correspondent first citation within the text.

The works published in Romanian will be written in Romanian, translated into English, and presented between parentheses.

In a reference, the following compulsory elements will be specified: the author(s) first name initials and family name, the title of the work, the printing house, the place and the year of the periodical in which it was published, the number (month), the volume (bold), the year, the paper first and last page, e.g., as follows.

[1] *L. Hong, L. Jun-zhou, B. WANG, H. Chao-xun, C. Jin-cao*. Multi-body dynamics simulation of hatch cover opening and closing device based on crank-linkage transmission. Ship Science and Technology, 2023, 45(16): 32-36.

[2] *B. B. Kosenok, B. V. Balyakin, N. I. Zhil'tsov*. Crank–rod mechanism for an internal combustion engine[J]. Russian Engineering Research,2017,37(1): 19-22.

[3] *H. Chunming, Z. Bo, L. Na, et al.* Air-fuel ratio control of two-stroke aviation piston engine[J]. Journal of Aerospace Power, 2023, 38（11）：2757-2765

[4] *Z. Sui, M. Qiang, Z Liang, et al.* Motion simulation design of crank-connecting rod mechanism of automobile engine [J]. Journal of Physics: Conference Series, 2021, 1798(1):012040-.

[5] *K. Chai, J. Lou, Y. Yang*. Mechanical Performance Analysis and Experimental Study of Four-Star-Type Crank-Linkage Mechanism[J].Applied Sciences,2023,13 (14):

[6] *T. Ren, S. D. Liao, T. W. Qin , et al.* Simulation and Parameter Optimization of the Crank-Slider Pumping Unit Based on ADAMS Virtual Prototyping Technology [J]. Advanced Materials Research,2013, 2228 (645-645): 497-500.

[7] *G. Q L, D. X W, B. Z G, et al.* Dynamics Simulation of the Crank and Connecting Rod Mechanism of Diesel Engine[J]. Advanced Materials Research,2011, 354-355(354-355):438-441.

[8] *M. Y. Shao, H. L. Wan*. Simulation on Vibration of Engine Crank-Connecting Rod Mechanism with Manufacturing Errors Using ADAMS[J]. Applied Mechanics and Materials,2010,1021(34-35):1088-1091

[9] *W. Rudolf, S. Michael, G. Peter, et al*. Experimental and Simulative Friction Analysis of a Fired Passenger Car Diesel Engine with Focus on the Cranktrain [J]. SAE International Journal of Engines,2016,9(4):2227-2241.

[10] *D. M W , Q. S ,M. K Z* , The Double Role Piston Pump Based on the Symmetrical Gears and Crank -Link-Slider Mechanism Driven by Servo Motor[J]. Applied Mechanics and Materials,2011,121-126 (121- 126):2308-2312.

[11] *T. Yuji, X. Yousheng, H. Xugang, et al.* A New Type of Inerter with Easily Adjustable Inertance and Superior Adaptability: Crank Train Inerter[J]. Journal of Structural Engineering, 2023,149(6)

[12] *Z. W H, C. J M, H. Z Y, et al*. Design analysis and application of a single gear double rack transmission structure [J]. Mechanical Research and Application. 2022,35(01):77-80.

[13] *P. Z H, D. W, R. X H, et al.* Mechanical analysis of transmission mechanism of 35 gear long ring rack pumping unit. [J]. Mechanical Transmission, 2023,47 (05):74-81.

[14] *Rucker Richard D.* An Analysis of the Parallel Combustion Two-Stroke Engine.SAE TECHNICAL PAPER SERIES,2000(1):1-15

[15] *N. Ziru, C. Da, L. Fuhui, et al.* Investigating tooth surface reconstruction principle of a gear rack and pinion system with variable transmission ratio pinion[J]. Proceedings of the Institution of Mechanical Engineers, Part C: Journal of Mechanical Engineering Science, 2024,238(12): 5976-5993.

[16] *K. J S, W. B S, L. Y Q.* Analysis on mechanical transmission efficiency of crank connecting rod mechanism[J]. Mechanical Science and Technology, 2008(03):347-350. ISSN: 1003-8728

[17] *W. Mengsheng, X. Nengqi, F. Minghui*. The torsional vibration simulation of the diesel engine crankshaft system based on multi-body dynamic model [J]. Proceedings of the Institution of Mechanical Engineers, Part K: Journal of Multi-body Dynamics, 2021,235(3): 443-451

[18] *B. S. Matekar, M. A. Fulambarkar*. Displacement analysis of slider in slider-crank mechanism with joint clearance[J].Australian Journal of Mechanical Engineering,2020,20(4):1-10.

[19] *Q. Xiao, S. Liu, A. Nie, et al.* Dynamic analysis of the moving mechanism of the reciprocating compressor with clearance joints[J]. Vibro engineering PROCEDIA, 2018, 1976-81.

[20] *Z. L C.* Research on dynamic performance of connecting rod and crankshaft of two-stroke engine based on co-simulation[D]. Inner Mongolia University of Science & Technology, 2022.
[21] *P. I Naeeni, A. Keshavarzi , I. Fattahi.* Parametric Study on the Geometric and Kinetic Aspects of the Slider-Crank Mechanism[J]. Iranian Journal of Science and Technology, Transactions of Mechanical Engineering,2019,43(3):405-417.
[22] *S. V M,Yu. S S ,V. L R , et al.* Method for Calculating the Counterweight Mass of a Crank-and-Rod Mechanism [J].Russian Engineering Research,2024,44(2):193-200.
[23] H. Wang, H. Hanz, C. Zhouy, et al. Load -bearing contact analysis of modified gear based on time-varying joint stiffness[J]. Modular Machine Tool & Automatic Manufacturing Technique,2024,(04):181-186+192.
[24] *M. Rahat I M, S. Bodzás*. An Analysis of Comparative Static Structural FEA for Spiral Bevel Gears with Various Tooth Angles and Loads[J]. Advances in Science and Technology, 2024,15339-46.
[25] *G. Shen, D. Xiang, N. Xie, et al.* Study on the Influence of Gear Rattling on Pitting Fatigue Failure[J]. Applied Mechanics and Materials,2014,2948 (496-500):634-641.
[26] *F. Concli, L. Fraccaroli*. Investigation of the Fatigue Strength Behaviour of a Fine 2 mm Module Gear[J].International Journal of Computational Methods and Experimental Measurements, 2023,11(2)
[27] *Q. Shao, K. Jiajie, X. Zhiguo, et al*. Effect of pulsed magnetic field treatment on the residual stress of 20Cr2Ni4A steel [J]. Journal of Magnetism and Magnetic Materials,2019,476: 218-2, PhD Thesis, Politehnica Bucharest, 2023.